WORD COUNT (main text) : 5078 words PAGE COUNT (all included) : 14.4 pages

Petrology of Indus River sands : a key to interpret erosion history of the Western Himalayan Syntaxis

Eduardo Garzanti[*1], Giovanni Vezzoli[1], Sergio Andò[1], Paolo Paparella[1], and Peter D. Clift[2]

[1] *Dipartimento di Scienze Geologiche,Università di Milano-Bicocca, 20126 Milano (Italy)*
Tel: (39) 2 64484338 Fax: (39) 2 64484273 E-mail: eduardo.garzanti@unimib.it

[2] *Department of Geology and Geophysics,* MS#22, *Woods Hole Oceanographic Institution, Woods Hole, MA 02543 (USA) Tel: (508) 2893437 Fax: (508) 4572187 E-mail: pclift@whoi.edu*

* *Corresponding author*

Keywords: Modern sands; Bulk petrography; Heavy minerals; Sediment budgets; Collision orogens; Karakorum; Nanga Parbat; Himalaya.

Abstract

The Indus River has been progressively transformed in the last decades into a tightly-regulated system of dams and channels, to produce food and energy for the rapidly growing population of Pakistan. Nevertheless, Indus River sands as far as the delta largely retain their distinct feldspar- and amphibole-rich composition, which is unique with respect to all other major rivers draining the Alpine-Himalayan belt except for the Brahmaputra. Both the Indus and Brahmaputra Rivers flow for half of their course along the India-Asia suture zone, and receive major contributions from both Asian active-margin batholiths and upper-amphibolite-facies domes rapidly exhumed at the Western and Eastern Himalayan syntaxes.

Composition of Indus sands changes repeatedly and markedly in Ladakh and Baltistan, indicating overwhelming sediment flux from each successive tributary as the syntaxis is approached. Provenance estimates based on our integrated petrographic-mineralogical dataset indicate that active-margin units (Karakorum and Transhimalayan arcs) provide ~81% of the 250±50 10^6 t of sediments reaching the Tarbela reservoir each year. Partitioning of such flux among tributaries and among source units allows us to tentatively assess sediment yields from major sub-catchments. Extreme yields and erosion rates are calculated for both the Karakorum Belt (up to 12,500±4700 t/km^2 yr and 4.5±1.7 mm/yr for the Braldu catchment) and Nanga Parbat Massif (8100±3500 t/km^2 yr and 3.0±1.3 mm/yr). These values approach denudation rates currently estimated for South Karakorum and Nanga Parbat crustal-scale antiforms, and highlight the major influence that rapid tectonic uplift and focused glacial and fluvial erosion of young metamorphic massifs around the Western Himalayan Syntaxis have on sediment budgets of the Indus system.

Detailed information on bulk petrography and heavy minerals of modern Indus sands not only represents an effective independent method to constrain denudation rates obtained from temperature-time histories of exposed bedrock, but also provides an actualistic reference for collision-orogen provenance, and gives us a key to interpreting provenance and paleodrainage changes recorded by clastic wedges deposited in the Himalayan foreland basin and Arabian Sea during the Cenozoic.

1. Introduction

The Himalaya and Karakorum are the archetype of orogenic belts produced by continental collision [1]. A complete transect across the collision zone, from the Asian active margin to the Indian passive margin, is exposed in the Western Himalayan Syntaxis [2,3]. In this area of extreme elevation and relief, rapid Plio-Quaternary uplift has resulted in spectacular unroofing of young (<10 Ma) migmatitic domes on both sides of the Tethyan suture [4-6].

Northern Pakistan thus represents a superb natural laboratory in which to study the relationships between active orogenic processes, erosion, and sediment composition (Fig. 1). Because of rapid transport from areas of high relief and negligible chemical weathering in arid climates, detrital signatures of river sands faithfully reflect the geology of source terranes.

This study describes the composition of Indus River sands, only scantily documented so far [7], and shows how high-resolution petrographic and heavy-mineral studies represent an effective way, complementary to geochemical and isotopic techniques [8,9], to investigate erosion patterns and sediment fluxes from the Himalayas. Understanding the modern erosion system will enhance our ability to interpret the provenance of ancient Indus Fan deposits [10], paleodrainage changes across the foreland basin [11,12], and unroofing history of the Western Himalayan Syntaxis during ongoing continental collision [13].

1.1 Sampling and analytical procedures

Very fine- to medium-grained sand samples were collected on active bars of the Indus River and its major tributaries across Pakistan in February 2001. Bedload samples from mountain tributaries draining specific source areas were also studied in order to identify the signatures of each major structural domain ("first-order sampling scale" of [14]). The complete set of 85 samples includes four eolian dunes from the Thal Desert (Fig. 1).

In each sample, 400 points were counted by the Gazzi-Dickinson method [15]. Thin sections were stained with alizarine red to distinguish dolomite and calcite. Detailed classification schemes [16] allowed us to collect full quantitative information on rock fragments, and to recalculate a spectrum of primary proportional and secondary ratio parameters (Table 1). In 71 samples, 200 to 250 transparent heavy minerals were counted on grain mounts. Heavy minerals were concentrated with sodium metatungstate

Table 1. Key Indices for Framework Composition and Heavy Mineral Suites.

Framework Composition (QFL%)	
Q	quartz
F	feldspars
Lv	volcanic and subvolcanic lithics
Lc	carbonate lithics (including marble)
Lp	terrigenous lithics (shale, siltstone)
Lch	chert lithics
Lm	metamorphic lithics
Lu	ultramafic lithics (e.g., serpentinite)
L = Lv + Lc + Lp + Lch + Lm + Lu = total lithic grains (crystal size <63 μm)	
Ratio parameters (%)	
P/F	plagioclase (excluding chessboard-albite) / total feldspars
Rcd/c	dolostone grains / total carbonate rock fragments
Rmb/m	metabasite grains / total metamorphic rock fragments
Heavy Minerals (HM%)	
ZTR	ultrastable minerals (zircon, tourmaline, rutile)
A	amphiboles
Px	pyroxenes
O + S	olivine + chrome spinel
LgM	low-grade minerals (mostly epidote-group minerals)
Gt	garnet
HgM	high-grade minerals (staurolite,andalusite,kyanite,sillimanite)
&	other minerals (mainly sphene)
HMC = weight percentage of heavy minerals in the 63-250 μm fraction	

Table 1 INDUS Garzanti et al.

(density 2.9 g/cm^3), using the 63-250 micron fraction treated with oxalic and acetic acids.

2. The Indus Basin

The Indus, one of the world's big rivers (~2900 km long; basin area ~10^6 km^2), flows from Tibet to the Arabian Sea mostly through arid lands, where the bulk of rainfall is brought in by the summer monsoon [17]. The urgent needs of a population with growth rates above 3% has led to intense exploitation of Indus waters, which provide 90% of Pakistan's agricultural requirements and 6000 MW of electricity. After the Indus Waters Treaty in 1960 gave rights to the entire flow of the Indus, Jhelum and Chenab Rivers to Pakistan, and of the Ravi, Beas and Sutlej Rivers to India, a system of large dams and link canals was built to irrigate arid plains and compensate for lost waters in eastern Pakistan [18].

2.1 Indus River upstream of Tarbela Dam

The Indus River rises from glaciers north of Mt.Kailas, and flows for a third of its course along the suture zone in southern Tibet. Next, it cuts deeply across the Western Himalayan Syntaxis, an area of extreme relief (five peaks above 8000 m, 68 above 7000 m) with more ice cover than any other extra-polar region [19]. Precipitation in the mountains is derived from atmospheric depressions moving from the west in winter and spring. Only occasionally does the monsoon extend sufficiently north to cause summer precipitation. High ablation rates in these large sub-tropical mountain glaciers lead to abundant supra-glacial debris and high sediment load of the ensuing melt streams. During summer, when snow melts, water discharge increases 20-50 times and sediment load 500-1000 times [20].

The Indus River is unregulated upstream of Tarbela Dam. Suspended loads of 287 to 323 10^6 t/yr were determined prior to 1974, when the dam was completed [17,21]. A suspended load of ~235 10^6 t/yr was estimated from a ~3.1 km^3 loss of gross storage capacity of Tarbela Lake during the subsequent 25 years, caused by accumulation of ~6 10^9 t of sediments [17]. Fluxes of only 200 10^6 t/yr are also reported [22,23].

2.2 Indus River downstream of Tarbela Dam

After construction of Tarbela Dam, sediment flux downstream dropped to 52 10^6 t/yr [17]. Even before, in this low-gradient tract the Indus River was depositing ~80 10^6 t/yr of sand, and showed a downstream

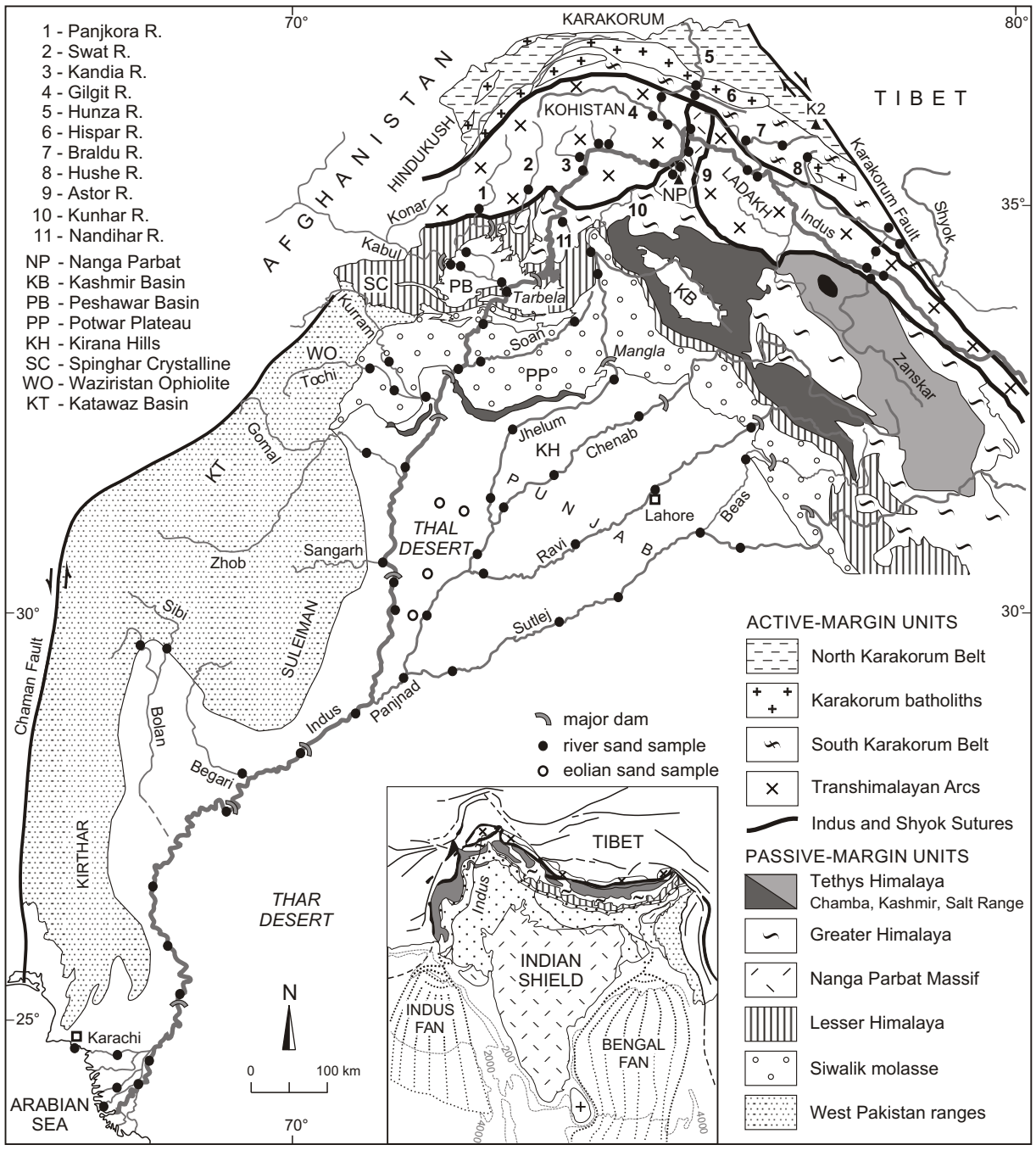

Figure 1 - INDUS Garzanti et al.

decrease in sediment discharge in spite of the ~37 10^6 t/yr supplied by the Kabul River [21]. Most of the Kabul load is provided by its Chitral-Konar tributary, draining the high-relief and snow-covered Hindukush Range; minor suspended load (1.2 10^6 t/yr) is carried by the Swat River, chiefly draining the Kohistan Arc [17]. Farther downstream, the Indus River enters a narrow gorge across the Potwar Plateau, and exits the Himalaya at the western tip of the Salt Range.

2.3. Indus River across the plains

In the hot dry Pakistan plains, rainfall is <300 mm/yr. Arid areas include the Thal Desert, a region of ~10,000 km^2 between the Indus and its Punjab tributaries, and the much wider Thar Desert, straddling the India/Pakistan boundary south of Punjab. Major tributaries draining the West Pakistan ranges are the Gomal (30 10^6 t/yr), characterized by extreme concentration of suspended solids, and the Kurram (3 10^6 t/yr [17]). Minor streams flow only during flash floods.

In a few decades, the Indus River has been effectively engineered into the largest integrated irrigation system in the world. Until 1947, the Indus load largely settled in the plains, whereas ~250 10^6 t/yr reached the delta and fostered rapid seaward growth (30 m/yr [21]). From 1932 to 1960, barrages built along the lower Indus River drastically reduced sediment discharge to the Arabian Sea to ≤50 10^6 t/yr. After 1960, all Punjab tributaries (Jhelum, Chenab, Ravi, Beas, Sutlej) have been dammed and linked by canals, and water discharge dropped sharply (from ≥100 to ≤60 km^3/yr). Flow in the Ravi and Sutlej Rivers ceased except during monsoon floods. Mangla Dam, completed in 1967, reduced sediment load of the Jhelum River from 45 to <0.5 10^6 t/yr [18,21].

3. Geology of the Western Himalaya Syntaxis

The formation of the Western Himalayan Syntaxis began at ~55 Ma, when the edge of the Indian passive margin underthrusted the Asian active margin [13,24]. The latter includes the Kohistan and Ladakh Arcs, delimited by the Indus Suture to the south and by the Shyok Suture to the north (Fig. 1; [25,26]). Farther north lie the Hindukush and Karakorum Ranges, which document active-margin evolution since the Early Jurassic [27]. The syntaxis is characterized by a series of actively-growing crustal-scale antiforms, which are oriented transverse to the Indus Suture on the Himalayan side (Nanga Parbat-Haramosh Massif

cut by the Indus River), but sub-parallel to it on the Karakorum side (Askole-Dassu-Mangol Bluk domes cut by the Braldu River and its Basha tributary [5,6]).

3.1 Karakorum and Hindukush

The Ordovician to Cretaceous North Karakorum sedimentary succession, exposed from the Hindukush to the Karakorum Fault and passing northwards to a belt of black slates, is affected by polyphase Tertiary deformation and very low-grade metamorphism [28,29]. The backbone of the Karakorum is represented by a calc-alkaline quartz diorite-granodiorite intruded during the mid-Cretaceous (95-110 Ma) [30]. The South Karakorum Belt displays a northeastward increase in metamorphism from structurally-lower phyllites, to staurolite metasediments, to sillimanite metasediments at the top. Its tectono-metamorphic evolution includes an early stage of crustal thickening and south-vergent thrusting sealed by ~37 Ma granites [31]. Crustal melting and leucogranite intrusions followed at 25-21 Ma (e.g., Baltoro Granite [31]). The subsequent indentation stage was characterized by dextral transpression in the Karakorum and sinistral transpression in the Hindukush. Exhumation of young (<10 Ma) sillimanite-bearing rocks and migmatites took place at peak rates up to 6 mm/yr [5,6,32].

3.2 Transhimalayan arcs and sutures

The Kohistan and Ladakh Batholiths are the dissected remnants of a magmatic arc fed by northward subduction of Neotethyan oceanic lithosphere during Cretaceous to Paleogene times [2].

The complete, northward-tilted lithospheric section exposed in southern Kohistan includes peridotites and granulite-facies metagabbros at the base. Amphibolite-facies metaigneous rocks (Kamila Amphibolite) and greenschist-facies metasediments (Gilgit Complex) are intruded by layered gabbronorites formed in the sub-arc magma chamber (Chilas Complex). The arc massif comprises gabbroic to granitic intrusions. Magmatic activity took place in distinct pulses, separated by collision of Kohistan with the Karakorum and closure of the Shyok Suture in the Late Cretaceous. Volcanic, volcaniclastic, and carbonate rocks mainly occur in the north [25].

The Ladakh Batholith includes olivine-norite to granitic intrusions. The forearc-basin succession includes Lower Cretaceous carbonates, volcaniclastic turbidites, syn-collisional Nummulite-bearing

clastics, and eventually post-collisional arkosic alluvial fans [33]. Basaltic to dacitic lavas, volcaniclastic turbidites, and ophiolitic mélanges with blueschists are exposed along the Indus Suture [34].

3.3 Northwestern Himalaya

The complete evolution of the Indian passive margin is recorded by the Proterozoic to Eocene Tethys Himalayan succession widely exposed in the Zanskar Synclinorium [35]. Final closure of the Neotethys Ocean and attempted subduction of thinned Indian continental crust at ~55 Ma is documented by the age of both syn-collisional sandstones and eclogites [24].

Nappe stacking in the late Paleogene culminated at 24-18 Ma by crustal melting and leucogranite intrusions in the topmost part of the Greater Himalayan inverted metamorphic sequence. This high-temperature event was associated with extension along the Zanskar Normal Fault in the north and thrusting along the Main Central Thrust in the south [36,37].

3.4. Nanga Parbat Massif

The Nanga Parbat half-window chiefly exposes tonalitic biotite gneisses representing protoliths of Precambrian Indian basement, flanked by Greater Himalayan and kyanite- to chlorite-bearing Tethys Himalayan units [38]. Thermal gradients of 60°C/Km are recorded within the top 3 km of this growing crustal-scale antiform, cored by high-grade rocks including cordierite migmatites and leucogranites as young as ≤3 Ma [39]. In this area, characterized by the greatest continental relief on Earth (~7000 m in ~20 km), high denudation rates (3-5 mm/yr [3,40,41]) are maintained by very fast fluvial incision [19,42]. Rapid Plio-Quaternary uplift was synchronous with subsidence of the Peshawar and Kashmir Basins on either side of the syntaxis [43].

3.5 Pakistan Himalaya

The Indian-margin sequence in northern Pakistan includes fold nappes of garnet-kyanite granitoid gneisses and metasediments, passing southward to greenschist-facies and unmetamorphosed strata [44,45]. Indian metamorphic rocks extend as far west as the Spinghar Crystalline in Afghanistan [46]. Tertiary foreland-basin sandstones are widely exposed from the Hazara syntaxis to the Potwar Plateau. The Himalayan front is represented by the Salt Range, including Paleozoic to Paleogene strata detached over

Eocambrian salt and uplifted in the latest Miocene [47]. Precambrian rocks of the Indian Shield are exposed in the Kirana Hills between the Jhelum and Ravi rivers.

3.6 West Pakistan ranges

Thin-skinned, festoon-shaped thrust belts of western Pakistan (Suleiman-Kirthar Ranges) formed as a consequence of oblique convergence between India and Asia, largely accommodated by the sinistral Chaman Fault [48]. East of the transform boundary, the rigid Katawaz Basin includes thick Eocene-lower Miocene remnant-ocean turbidites [49]. Indian passive-margin strata of Jurassic and Cretaceous age are exposed further east. Supra-subduction ophiolites (Waziristan, Zhob, Muslimbagh, Bela) were obducted onto this succession around the Cretaceous/Tertiary boundary [50]. Tertiary strata include ophioliticlastic mudrocks, overlain by limestones, and finally by Neogene sandstones and conglomerates [51].

4. Composition of Indus Sands

4.1 Karakorum and Hindukush tributaries

The Indus River receives abundant detritus from the Karakorum and Hindukush via four major right-bank tributaries. Composition ranges from plutoniclastic (Hushe sand, derived from granodioritic batholiths and Baltoro Granite) to metamorphiclastic with dolomitic marble grains (Braldu and Hispar sands, largely derived from the South Karakorum), or may include common sedimentary to metasedimentary grains from very-low grade cover rocks (Hunza and Kabul sands, derived from North Karakorum and Hindukush, respectively). Heavy minerals include abundant to dominant blue-green to subordinately green and brown hornblende, associated with epidote, garnet, sphene, diopside, and minor staurolite and sillimanite (Fig. 2).

4.2 Ladakh and Kohistan tributaries

The Ladakh Batholith sheds pure arkosic detritus, with dominant blue-green and subordinately brown hornblende (Table 2). The Kohistan crustal sequence also provides abundant prasinite, epidosite, and amphibolite grains. Heavy-mineral assemblages are dominated by mainly blue-green hornblende, and include epidote, hypersthene, and clinopyroxenes; trace glaucophane and diallage are derived from blueschist ophiolitic mélanges marking the suture zone (Swat and Panjkora Rivers; [52]). Metabasite

Table 2. Petrography and mineralogy of modern Indus sands.

		% QFL														% HM							
	N	Q	F	Lv	Lc	Lp	Lch	Lm	Lu	tot	P/F	Rcd/c	Rmb/m	HMC	ZTR	A	Px	O+S	LgM	Gt	HgM	&	tot
ASIAN ACTIVE MARGIN																							
Hindukush	2	39	18	0	13	7	0	23	0	100	49	62	11	6,4	1	56	7	0	24	10	3	0	100
North Karakorum	1	23	23	0	18	13	0	24	0	100	67	61	5	2	5	66	2	0	20	2	0	4	100
Central Karakorum	2	50	46	0	2	0	0	2	0	100	63	n.d.	13	2,6	7	67	1	0	11	2	1	10	100
South Karakorum	3	53	32	0	10	0	0	4	0	100	49	59	10	5,4	5	45	6	0	21	13	2	7	100
Ladakh batholith	2	38	56	1	1	1	1	3	0	100	64	n.d.	20	20,5	1	83	5	0	6	1	0	3	100
Kohistan batholith	3	30	36	1	1	1	0	30	1	100	85	n.d.	52	32,8	1	68	10	0	22	0	0	0	100
INDIAN PASSIVE MARGIN																							
Greater Himalaya	2	57	25	0	7	0	0	11	0	100	54	23	9	4,1	8	44	5	0	8	18	15	1	100
Nanga Parbat	3	47	45	0	2	0	0	5	0	100	52	n.d.	7	6,8	2	63	8	0	9	13	1	3	100
Soan River	2	49	13	1	10	12	4	10	0	100	44	11	25	4,2	4	10	0	0	75	10	0	0	100
Jhelum River	2	39	10	2	14	13	1	20	0	100	58	36	12	7,0	1	27	3	0	25	42	0	1	100
Chenab River	2	53	17	1	4	7	0	18	0	100	48	64	7	2,2	5	23	2	0	23	34	12	0	100
Ravi River	2	56	10	1	2	14	0	17	0	100	44	n.d.	5	1,0	13	18	2	0	48	14	3	2	100
Sutlej River	3	58	15	1	11	6	0	8	0	100	40	14	7	3,9	12	33	3	0	14	26	10	2	100
WEST PAKISTAN RANGES																							
Suleiman Tributaries	6	34	9	4	21	10	4	12	5	100	60	13	27	10,1	7	18	17	4	36	14	2	1	100
Kirthar tributaries	2	19	4	0	66	4	2	6	0	100	53	9	7	0,3	15	7	7	4	45	16	2	4	100
TRUNK RIVER																							
Indus upstream Zanskar	1	38	19	0	7	22	0	12	1	100	67	25	9	1,9	5	56	4	1	29	3	0	2	100
Indus pre-Tarbela	2	44	31	0	10	3	0	11	0	100	54	45	28	13,1	1	54	11	0	15	13	4	2	100
Indus pre-Punjab	2	42	23	2	12	5	1	15	1	100	59	56	26	10,4	1	52	6	0	29	8	3	1	100
Indus delta	5	47	19	0	13	3	1	16	0	100	57	33	23	9,9	3	50	5	0	24	12	4	2	100
THAL DESERT	4	37	34	1	7	3	0	18	0	100	51	42	32	20,4	2	56	10	0	17	12	2	1	100

detritus is most abundant in Kandia River sand, which contains brown hornblende from the granulite-facies Chilas Complex, and epidote and actinolite from the greenschist-facies Gilgit Complex.

The Shyok and Gilgit Rivers, draining both sides of the Shyok Suture, carry quartz, feldspars, sedimentary, and metamorphic lithic grains from the Karakorum and Transhimalayan Arcs. Heavy-mineral assemblages are hornblende-dominated. The Astor River, draining both the Nanga-Parbat Massif and Ladakh Arc, carries high-rank quartzofeldspathic sands with dominant blue-green hornblende.

4.3 Himalayan tributaries

Upstream of Tarbela Dam, the Indus River receives detritus from the north side of the Himalaya (Zanskar River), runs across the Nanga Parbat Massif, and finally cuts through the Himalayan Belt. Detritus from the Greater Himalaya is high-rank metamorphiclastic (Zanskar, Nandihar Rivers), including blue-green to subordinately green and brown hornblende, garnet, staurolite, kyanite, sillimanite, epidote, and ultrastables. The Nanga Parbat Massif sheds very-high-rank quartzo-feldspathic detritus including mainly blue-green to brown hornblende and subordinate garnet, epidote, and diopside.

The Soan River, exclusively draining Tertiary foreland-basin units across the Potwar Plateau, carries polycyclic sands including shale/slate, sandstone/metasandstone, and calcareous grains, and a few chert and volcanic grains; heavy minerals are epidote-dominated, with minor garnet, hornblende, and ultrastables. The Himalayan tributaries of Punjab carry quartzolithic sands including sedimentary (carbonate, shale/sandstone) and metasedimentary grains, with rare chert and volcanic grains. The Chenab and Sutlej sands are richer in feldspars, high-rank metamorphic grains, kyanite, and sillimanite; the Jhelum and Ravi sands are richer in shale/slate grains and epidote-group minerals.

4.4 West Pakistan tributaries

Rivers of west central Pakistan carry lithic sands with abundant sedimentary and low-rank metasedimentary grains (limestone, shale/slate, sandstone/metasandstone, chert). Heavy minerals, including epidote, garnet, commonly rounded ultrastables, red to coffee-brown chrome spinel, and staurolite, are largely recycled from terrigenous units. The Kurram River also carries K-feldspar and blue-green hornblende from the Spinghar Crystalline. The Tochi River carries abundant ultramafic, volcanic, metabasite, and plagioclase grains, along with augite, diopside, enstatite, olivine, and trace glaucophane

from the Waziristan Ophiolite. Rivers of southern Pakistan carry purely sedimentaclastic detritus, either dominated by limestone grains (Bolan River) or including recycled quartz and feldspars (Sibi River).

These distinct lithic signatures become homogenized across the plains, where quartz sharply increases, suggesting recycling of accreted foreland-basin units or alluvial sediments (Kurram, Gomal, Sangarh Rivers). Sharp increases in hornblende in Kurram and Begari River sands just upstream of the confluence indicates mixing with Indus sediments. Only a few volcanic to ultramafic grains, pyroxenes and chrome spinel persist in the lower tract of the Kurram and Gomal Rivers, indicating negligible contributions from western Pakistan ophiolites to the Indus sands.

4.5 Trunk river

The Indus River in Ladakh carries carbonate and shale/slate grains from sedimentary to low-rank metasedimentary cover rocks, quartz and feldspars from the Ladakh Arc, and rare ultramafic grains; heavy minerals are mostly blue-green hornblende and epidote. Downstream of the Zanskar confluence, sands are enriched in quartz, K-feldspar, carbonate and high-rank metamorphic grains, as well as in garnet and sillimanite from Greater Himalayan units.

Indus sands in Baltistan are enriched first in feldspars and blue-green hornblende from Jurassic to Miocene plutons of the Asian active margin (Hushe/Shyok River), and next in metamorphiclastic detritus including marble, hornblende, and epidote from the South Karakorum Belt (Braldu/Shigar River).

Next, the river cuts across the Nanga Parbat Massif, the Kohistan Arc, and the Himalaya. Increases in dolostone and metabasite grains reflect supply from Karakorum and Kohistan sources. Blue-green hornblende prevails over epidote, clinopyroxenes, and hypersthene from arc rocks, as well as garnet, kyanite, and staurolite from amphibolite-facies Karakorum and Himalayan units.

Across the Potwar Plateau and downstream of the Soan-Indus confluence, composition is influenced by recycling of Tertiary foreland-basin sediments. The Q/F ratio increases, along with sedimentary (limestone, shale/sandstone, chert), very-low rank metasedimentary, volcanic, and epidote grains.

The Q/F ratio, limestone and very low-rank metasedimentary grains tend to increase further downstream of the confluence with Punjab tributaries and in deltaic sands. Garnet and kyanite are more common locally, indicating subordinate supply from Himalayan sources.

4.6 Thal Desert

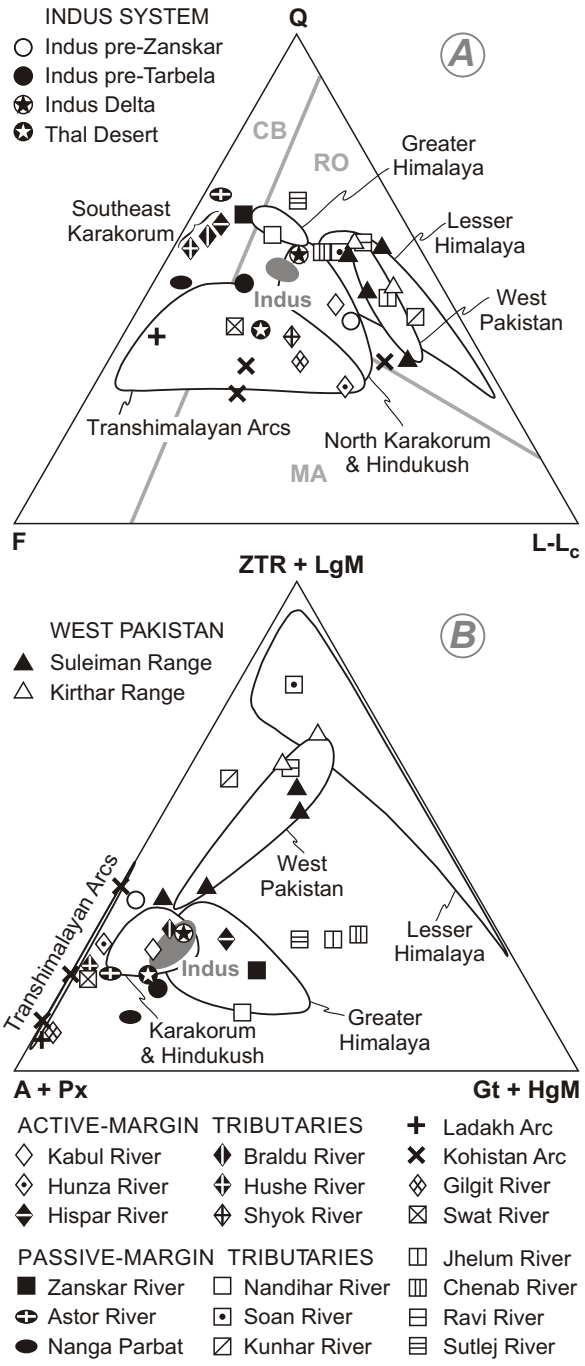

Figure 2 - INDUS Garzanti et al.

Dune sands have low Q/F ratio (~1) and abundant metabasite grains, indicating major contributions from the Kohistan Arc. Concentrated heavy-mineral assemblages include dominant blue-green hornblende, epidote, garnet, augite, diopside, and hypersthene.

5. Sediment budgets

Terrigenous fluvial sediments are complex mixtures of monocrystalline and polycrystalline grains eroded from many different lithological and tectonic units, and supplied in various proportions by numerous streams to successive segments of a trunk river system. If the end-member compositional signatures of detritus derived from each main geological unit and carried by each main tributary are known, the relative contribution from each of these sources to the total sediment load can be quantified mathematically with forward mixing models [53]. This method, described in detail in Appendix A3 (available in the online edition of EPSL and from the EPSL Data Depository upon request), allows us to partition the total sediment flux, and thus to obtain independent estimates of sediment yield and denudation rates from various sub-catchments [54,55].

Relative contributions from various detrital sources are assessed from an integrated petrographic-mineralogical dataset of up to fifty compositional parameters, and are thus precise in theory. In practice these calculations are non-unique and uncertain, being affected by numerous sources of potential error. In order to verify outcome sensitivity, several sets of independent trials were carried out according to a range of different assumptions, and the mean and the standard deviation of the results obtained were calculated. A further way to test the results for consistency, and to obtain more accurate estimates, is to perform separate complementary sets of calculations for bulk petrography and heavy minerals. Although commonly influenced by local effects and imperfect mixing [55,56], simple calculations on terns of samples collected upstream and downstream of major confluences provide additional help to constrain total sediment budgets (Fig. 3). Duplicate samples collected in different periods of time in the same place, or at a distance along the same river, represent a further effective way to minimize various sources of error.

Although we tried and use as large a sample set as possible and to consider all of the direct information available on sediment load, the sediment budgets of the Indus system presented herein should be considered as tentative. They suffer from intrinsic variability of natural phenomena and difficulties in collecting

duplicate samples from remote areas. They are based on data from bedload sands, and may not be applicable to the mud-rich suspended-load fraction. And they are based on several assumptions which are never strictly verified, including lack of chemical dissolution, mechanical destruction, compositional fractionation, grain-size effects and changes in sediment textures, cross-channel heterogeneities, sediment storage, and recycling. In mountain catchments, rapid recycling of Pleistocene glacial deposits may lead to anomalous sediment fluxes and overestimated rates of bedrock erosion. In the plains, particularly in tightly-regulated systems such as the Indus where sites of deposition and erosion are largely determined by human activities (e.g., reservoirs), fluvial transport is anything but steady state, compositional trends are commonly irregular, and provenance estimates become most uncertain.

5.1 Heavy-mineral concentrations

Heavy minerals, even though influenced by hydraulic sorting, provide crucial provenance information. Their concentration varies strongly in detritus derived from different geological units or carried by different tributaries, and this must be carefully taken into account when calculating provenance of bulk sediments from heavy-mineral data [57]. Heavy minerals are much more abundant in detritus from the Ladakh and Kohistan Arcs (29±9%) than in detritus from Karakorum-Hindukush (5±2%), Nanga Parbat (7±6%), and Himalayan units (5±3%). Heavy minerals are scarce in sands from thin-skinned West Pakistan ranges (2±2%), with the exception of ophioliticlastic sands carried by the Tochi River (21±3%). Indus sands are rich in heavy minerals (11±7%), but not as rich as Thal Desert dunes (20±6%).

5.2 Indus sands upstream of Tarbela Dam

Major compositional changes of Indus sands downstream of the Zanskar, Shyok/Hushe, and Braldu/Shigar confluences indicate overwhelming sediment contribution from each successive tributary as the syntaxis is approached (Fig. 3). Even extreme compositions are observed locally (Indus sand downstream of its Braldu/Shigar confluence is virtually pure Shigar sand; Gilgit sand downstream of its Hunza confluence is virtually pure Hunza sand), which may be ascribed to several processes, including imperfect mixing, seasonal variations in relative sediment discharge, different grain-size distributions of tributary and trunk-river sediments, alluvial-fan growth at confluences, and reworking of Quaternary terraces and glacial deposits.

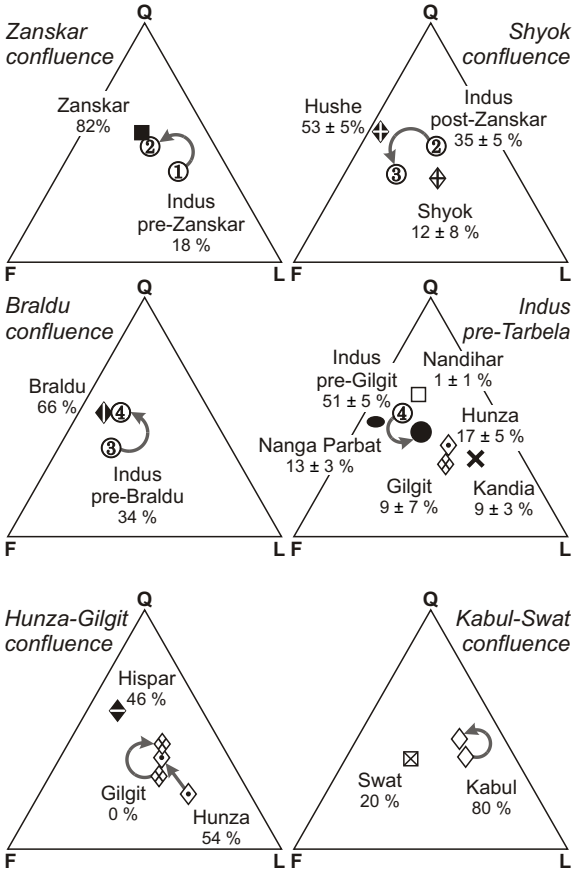

Figure 3 - INDUS Garzanti et al.

The overall bulk-sediment budget calculated from our integrated petrographic-mineralogical dataset indicates that active-margin units provide 81±2% of the Indus bedload entering Tarbela Lake (60±6% from Karakorum; 6±4% from the Ladakh Arc and South Tibet; 14±4% from the Kohistan Arc), with the remaining 19±2% accounted for by Himalayan units (Nanga Parbat 13±3%; Tethys and Greater Himalaya 6±3%). Half of total pre-Tarbela flux is contributed by two Karakorum tributaries, the Braldu/Shigar (34±6%) and Hunza Rivers (17±5%).

5.3 Sediment yields and erosion rates

Sediment flux entering Tarbela Lake (250±50 10^6 t/yr [17,21-23]) can be partitioned according to our provenance estimates. These imply sediment yields of 6000±1800 t/km^2 yr for Karakorum (~25,000 km^2), 130±100 t/km^2 yr for the Ladakh Arc and South Tibet (~120,000 km^2), 1400±700 t/km^2 yr for the Kohistan Arc (~25,000 km^2), 8100±3500 t/km^2 yr for the Nanga Parbat Massif (~4000 km^2), 600±400 t/km^2 yr for the Tethys and Greater Himalaya (~25,000 km^2).

By assuming a mean rock density of 2.75 g/cm^3 [22], we calculated average erosion rates of 2.2±0.7 mm/yr for Karakorum, 0.05±0.05 mm/yr for the Ladakh Arc and South Tibet, 0.5±0.2 mm/yr for the Kohistan Arc, 3.0±1.3 mm/yr for the Nanga Parbat Massif, and 0.2±0.1 mm/yr for the Tethys and Greater Himalaya. The highest sediment yields and erosion rates are obtained for the Braldu/Shigar (12,500±4700 t/km^2 yr; 4.5±1.7 mm/yr) and Hispar catchments (11,000±5000 t/km^2 yr; 4.0±1.8 mm/yr), both draining the South Karakorum Belt northeast and north of Nanga Parbat. Much lower values are estimated for the upper Hunza basin in the North Karakorum (2500±1600 t/km^2 yr; 0.9±0.6 mm/yr).

Our estimates match the lower end of the range of denudation rates calculated from temperature-time histories of bedrock exposed in the Nanga Parbat (3–4 mm/yr [40,41]) and South Karakorum domes (~5 mm/yr [6]). They are also compatible with the sediment yields measured for the Hunza River (5000–8000 t/km^2 yr [20]), and for the Chitral/Konar River draining the Hindukush (1842 t/km^2 yr [17]).

This set of estimated sediment yields indicates that erosion rates decrease exponentially eastward, northward, and westward away from the sharp peak recorded in the syntaxis region. This parallels the exponential increase of apatite fission-track ages observed away from the rapidly-exhuming domes of the Western Himalayan Syntaxis [4].

5.4 Indus sands downstream of Tarbela Dam

Sediment-budget calculations are of limited value downstream of Tarbela Dam, where sediment discharge has been profoundly modified and virtually stopped by man. Bulk petrography and heavy minerals of Indus sands downstream of the Kabul confluence are very close to Kabul sands, reflecting effective sequestration of Indus sediments in Tarbela Lake. Farther downstream, feldspars remain relatively scarce and the pre-Tarbela composition is never restored. Detrital modes of Indus sands at the Salt Range front reflect extensive recycling of older (pre-dam) Indus sediments (54±3%), with subordinate contributions from Kabul (33±2%), Soan (11±2%), and other tributaries draining the West Pakistan ranges (3±2%; Kurram, Tochi, Gomal, Sangarh Rivers).

5.5 Himalayan tributaries of Punjab

Large dams and link canals built since 1960 have hampered sediment transit across the Punjab. As a consequence, the composition of river sand may vary erratically (e.g., detrital modes of one Ravi sample are very close to Chenab sand). Bulk petrography and heavy minerals of Jhelum sand change markedly downstream of Mangla Dam, testifying to extensive recycling of locally-exposed foreland-basin sediments, but are restored farther downstream, pointing to erosion of older (pre-dam) bank and channel sediments. Garnet tends to be more abundant in samples with higher heavy-mineral concentration ($r = 0.53$, probability 5%), suggesting local hydraulic-sorting effects. Anomalous compositions (higher feldspars, amphiboles, and pyroxenes) are observed all along the eastern edge of the Thal Desert from upstream of the Jhelum-Chenab confluence to the Indus-Panjnad confluence, revealing mixing with eolian sands (locally >20% of river bedload).

Bulk bedload contributions of 15±6% from the Jhelum, 33±7% from the Chenab, 4±4% from the Ravi, 40±8% from the Sutlej, and 9±3% from the Thal dunes are tentatively estimated from our dataset. Overall bulk contribution from Himalayan-derived Punjab tributaries to the total Indus sediment budget is estimated at 39±4%.

5.6 The effect of chemical weathering

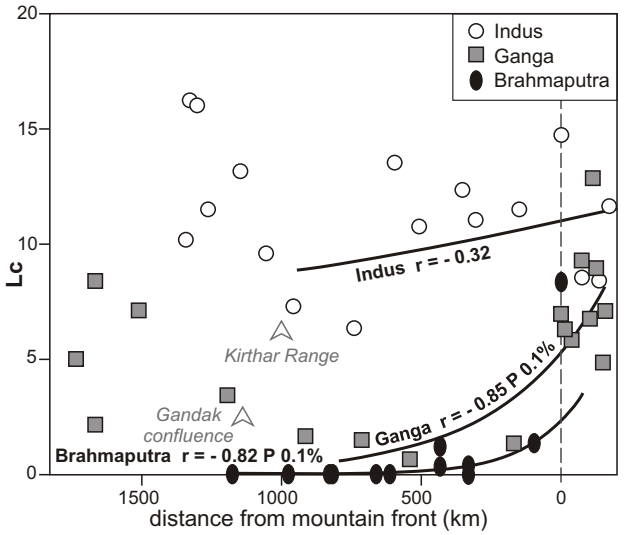

Figure 4 - INDUS Garzanti et al.

Contrary to what is observed for other big Himalayan rivers draining areas with heavier summer-monsoon rains, the abundance of carbonate grains in Indus sands does not decrease significantly across the arid plains of Pakistan (Fig. 4). Limestone rock fragments even increase in the lowermost reaches, because of local supply from the Kirthar Range. Pyroxenes (and even olivine, found in trace down to the delta) only locally show selective alteration and do not appear to be significantly depleted. In spite of extensive recycling of older sediments, largely induced by human activities, chemical weathering does not significantly affect the composition of Indus sands and was neglected in sediment-budget calculations.

5.7 Total Indus budget

From our integrated petrographic-mineralogical dataset, we calculate a bulk bedload contribution of 47±2% from active-margin units (27±3% from Karakorum, 10±3% from Hindukush, 3±2% from the Ladakh Arc and South Tibet, 7±2% from the Kohistan Arc) and 53±2% from Himalayan passive-margin units (including 39±4% from Punjab tributaries and 6±3% from Nanga Parbat) to the overall Indus flux. Our estimates are consistent with those based on geochemical signatures, which indicate important supply from the South Karakorum Belt, with contributions from Nanga Parbat limited to 5±3% [8,9].

However, erosion patterns deduced from modern sediments may not be extrapolated even to the recent past, and not only because of extensive human modifications of sediment fluxes. Petrographic and geochemical data from Indus Fan turbidites (higher feldspars and amphiboles, and less negative εNd values than deltaic sands [10,58-60]) suggest significantly greater contributions from active-margin units in pre-Holocene times. This is consistent with the peculiar composition of Thal Desert sands, interpreted here as originally transported by a paleo-Indus system characterized by different erosion and/or drainage patterns. It is possible that detritus now stored in the Thal Desert was largely generated originally from the huge sediment fluxes produced during glacier retreat at the beginning of the Holocene.

6. Symmetries of Himalayan Sediment Transport

The two big Himalayan river systems, the Indus and the Brahmaputra, show specular symmetry, a consequence of geometry and rheology of colliding continents (Fig. 5; [61]). Sourced in arid elevated lands of South Tibet, they run in opposite directions along the Indus-Tsangpo Suture, cut impressive gorges

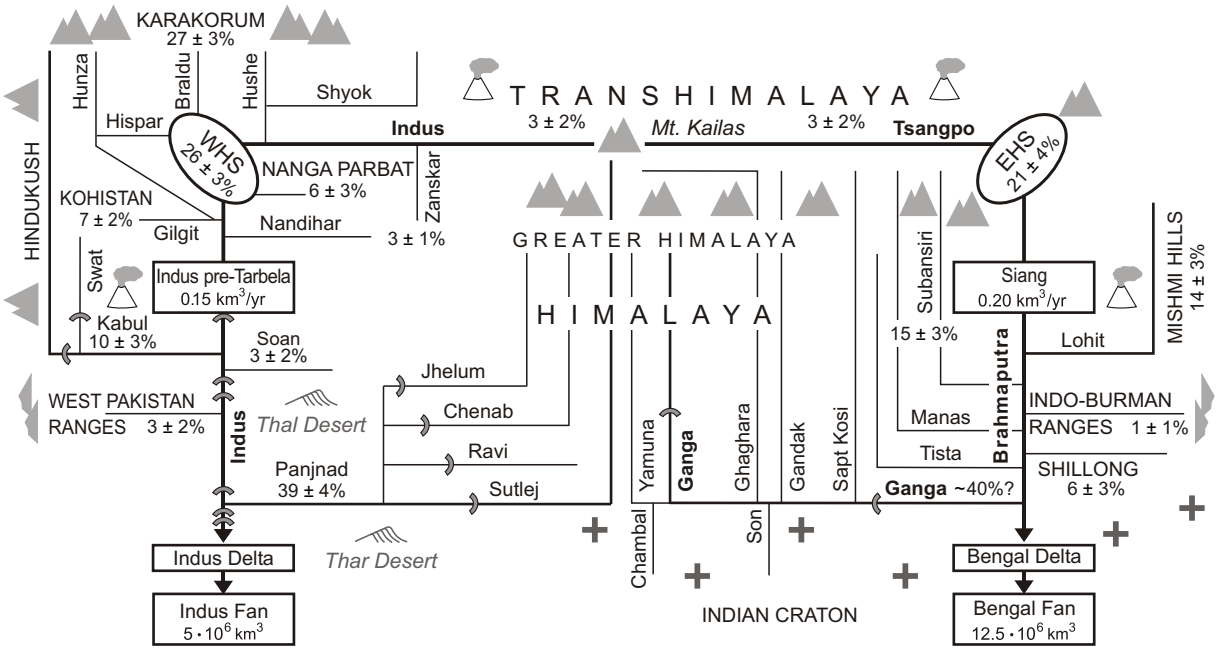

Figure 5 - INDUS Garzanti et al.

through growing crustal-scale antiforms at the two extremes of the Himalaya, and finally flow across the foreland and drop their load in the largest submarine fans on Earth. Major differences are related to climatic conditions (the monsoon-drenched Assam plains contrasting sharply with Pakistan deserts), and to human activities (the Brahmaputra being still a natural system whereas the Indus is strongly managed).

In both systems, the contribution from the vast elevated Tibetan lands is irrelevant to final composition. Crucial, instead, is the supply from young metamorphic massifs at the syntaxes, where relief and erosion rates are extreme, and sediment yields therefore huge. Higher, extensively-glaciated topography characterizes the Western Syntaxis, where migmatitic domes are rapidly exhumed both north and south of the suture zone [4]. Because the Himalayan part of the syntaxis (Nanga Parbat Massif) is small, Asian active-margin units provide the bulk of Indus sediments upstream of Tarbela Lake. Conversely, the Eastern Syntaxis is dominated by the broad Namche Barwa Massif, and Brahmaputra sands display a Greater Himalayan signature [54,62]. Similar average sediment yields (~1250 t/km^2 yr) and erosion rates (~0.5 mm/yr) are calculated for the Indus and Brahmaputra catchments upstream of the Himalayan front.

As the Brahmaputra receives significant contributions from left-bank tributaries draining Asian active-margin units in upper Assam (Lohit River) and finally from several right-bank Himalayan tributaries across the foreland including the Ganga, so the Indus is joined from the west by the Kabul River draining Hindukush and Kohistan and finally from the east in Punjab by Himalayan tributaries including the Sutlej. Contrary to both Ganga and Brahmaputra systems, which drain the northern Indian Shield and the elevated Shillong plateau, the Indus lacks cratonic sources.

In the end, Indus and Brahmaputra sands display common petrographic (abundant feldspar and metabasite grains) and mineralogical features (rich, amphibole-dominated assemblages), which are not shared by any other major river draining the Himalaya or the Alps (Fig. 6A; [63]). Such a peculiar signature reflects major contributions from both active-margin batholiths (10–15%) and upper-amphibolite-facies mid-crustal rocks rapidly unroofed at the syntaxes (20-25%), two sources which are unique to the Brahmaputra and Indus systems (Fig. 6B). Overall, Asian active-margin units supply only a sixth of the total Ganga-Brahmaputra flux [54], but nearly half of the total Indus budget.

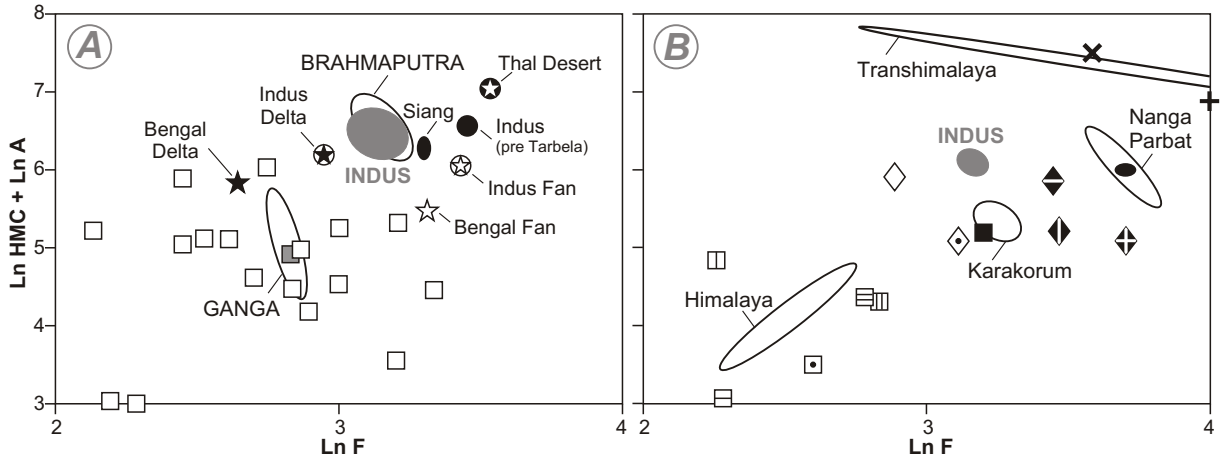

Figure 6 - INDUS Garzanti et al.

7. Conclusions

Modern Indus sediments consist of quartzo-feldspathic detritus from Transhimalayan batholiths and upper-amphibolite-facies domes rapidly uplifted on both Karakorum and Himalayan sides of the Western Himalayan Syntaxis, and of quartzolithic detritus from the Himalayan Belt (largely contributed by Punjab tributaries). Eolian (Thal Desert) and turbidite (Indus Fan) sands are characterized by even lower quartz/feldspar ratios than sands of the modern river system [60], reflecting only in part post-dam changes to sediment fluxes downstream of Tarbela Lake. Contributions from active-margin sources must have dominated for most of the Quaternary and Cenozoic [10].

Detritus generated in the Indus mountain catchment and accumulating in Tarbela Lake is mostly derived from active-margin units north of the Indus Suture. The largest load comes from the Braldu/Shigar River (85±30 10^6 t/yr), originating from the Baltoro Glacier and cutting across active migmatitic domes of the South Karakorum [5,6]. Erosion rates are estimated to exceed 4 mm/yr along the South Karakorum Belt northeast of the Nanga Parbat indenter, and to decrease exponentially eastward, northward, and westward away from the syntaxis. In the same directions fission-track ages show a parallel, exponential increase, reflecting exponentially decreasing exhumation rates [4].

The major impact of focused glacial and fluvial erosion of young metamorphic massifs on sediment budgets of big Himalayan rivers confirms that positive feedback between endogenetic tectonic forces and exogenetic erosional agents [3,37] plays a critical role in shaping the evolution of collision orogens and associated sedimentary basins.

Acknowledgments

The paper benefited from precious advice by B.Lombardo and A.Zanchi, and by careful reviews by H.von Eynatten and R.J.Wasson. Many hearty thanks to G.Ghielmi and F.Lazzati, who collected river sands all around Pakistan, and to J.Blum, Y.Najman, M.Searle, and H.Sinclair, who provided crucial samples from mountain rivers. G.Ghielmi determined areal distribution of geological units around the Western Himalayan Syntaxis by GIS techniques. Financial support by FIRB 2002 and PRIN 2003 to E.Garzanti.

References

[1] K.V. Hodges, Tectonics of the Himalaya and southern Tibet from two perspectives, Geol. Soc. Am. Bull. 112 (2000) 324-350.

[2] M.P. Searle, M.A. Khan, J.E. Fraser, S.J. Gough, M.Q. Jan, The tectonic evolution of the Kohistan-Karakoram collision belt alongthe Karakoram Highway transect, north Pakistan, Tectonics 18 (1999) 929-949.

[3] P.K. Zeitler, A.S. Meltzer, P.O. Koons, D. Craw, B. Hallet, C.P. Chamberlain, W.S.F. Kidd, S.K. Park, L. Seeber, M. Bishop, J. Shroder, Erosion, Himalayan geodynamics,and the geomorphology of metamorphism, GSA Today 11 (2001) 4-9.

[4] P.K. Zeitler, Cooling history of the NW Himalaya, Pakistan, Tectonics 4 (1985) 127-151.

[5] Y. Lemennicier, P. Le Fort, B. Lombardo, A.Pêcher, F. Rolfo, Tectonometamorphic evolution of the central Karakorum (Baltistan, northern Pakistan), Tectonophysics 260 (1996) 119-143.

[6] Y. Rolland, G. Mahéo, S. Guillot, A. Pêcher, Tectono-metamorphic evolution of the Karakorum Metamorphic complex (Dassu-Askole area, NE Pakistan): exhumation of mid-crustal HT-MP gneisses in a convergent context. J. Metam. Geol. 19 (2001) 717-737.

[7] P.E. Potter, Petrology and chemistry of modern big river sands, J. Geol. 86 (1978) 423-449.

[8] P.D. Clift, J.I. Lee , P. Hildebrand, N. Shimizu, G.D. Layne, J. Blusztajn, J.D. Blum, E. Garzanti E., A.A. Khan, Nd and Pb isotope variability in the Indus River system: implications for sediment provenance and crustal heterogeneity in the Western Himalaya, Earth Planet. Sci. Lett. 200 (2002) 91-106.

[9] J.I. Lee, P.D. Clift, G. Layne, J. Blum, A.A. Khan, Sediment flux in the modern Indus River inferred from the trace element composition of detrital amphibole grains, Sedim. Geol. 160 (2003) 243-257.

[10] P.D. Clift, N. Shimizu, G.D. Layne, J.S. Blusztajn, C. Gaedicke, H.-U. Schlüter, M.K. Clark, S. Amjad, Development of the Indus Fan and its significance for the erosional history of the western Himalaya and Karakoram, Geol. Soc. Am. Bull. 113 (2001) 1039-1051.

[11] P.F. Cerveny, N.M. Johnson, R.A.K. Tahirkheli, N.R. Bonis, Tectonic and geomorphic implications of Siwalik Group heavy minerals, Potwar Plateau, Pakistan, Geol. Soc. Am. Spec. Pap. 232 (1989) 129–136.

[12] Y. Najman, E. Garzanti, M. Pringle, M. Bickle, J. Stix, I. Khan I., Early Miocene paleodrainage and tectonics in the Pakistan Himalaya, Geol. Soc. Am. Bull. 115 (2003) 1265-1277

[13] E. Garzanti, S. Critelli, R.V. Ingersoll, Paleogeographic and paleotectonic evolution of the Himalayan Range as reflected by detrital modes of Tertiary sandstones and modern sands (Indus transect, India and Pakistan), Geol. Soc. Am. Bull. 108 (1996) 631-642.

[14] R.V. Ingersoll, A.G. Kretchmer, P.K. Valles, The effect of sampling scale on actualistic sandstone petrofacies, Sedimentology 40 (1993) 937-953.

[15] W.R. Dickinson, Interpreting provenance relations from detrital modes of sandstones, in: G.G. Zuffa (Ed.), Provenance of arenites, Dordrecht, Reidel, ASI Series 148, 1985, pp.333-361.

[16] E. Garzanti, G. Vezzoli, A classification of metamorphic grains in sands based on their composition and grade, J. Sedim. Res. 73 (2003) 830-837.

[17] S.S. Rehman, M.A. Sabir, J. Khan, Discharge characteristics and suspended load from rivers of Northern Indus Basin, Pakistan, Geol. Bull. Univ. Peshawar 30 (1997) 325-336.

[18] A. Meadows, P. Meadows, The Indus River – Biodiversity, Resources, Humankind, Oxford Univ. Press, 1999, 441 pp.

[19] J.F. Shroder, M.P. Bishop, Unroofing of Nanga Parbat Himalaya, in: M.A. Khan, P.J. Treloar, M.P. Searle, M.Q. Jan (Eds.), Tectonics of the Nanga Parbat Syntaxis and the western Himalaya, J. Geol. Soc. London Spec. Publ. 170, 2000, pp. 163-179.

[20] R.I. Ferguson, Sediment load of the Hunza River, in: K.J. Miller (Ed.), The International Karakoram Project, Cambridge Univ. Press 2, 1984, pp. 581-598.

[21] J.D. Milliman, G.S. Quraishee, M.A.A. Beg, Sediment discharge from the Indus River to the ocean: past, present, and future, in B.U. Haq, J.D. Milliman (eds.), Marine geology and oceanography of the Arabian Sea and coastal Pakistan, Van Nostrand Reynolds, New York, NY, 1984, pp. 65-70.

[22] G. Einsele, M. Hinderer, Terrestrial sediment yield and the lifetimes of reservoirs, lakes, and larger basins. Geol. Rundsch. 86 (1997) 288-310.

[23] E.L. Tate, F.K. Farquharson, Simulating reservoir management under the threat of sedimentation: the case of Tarbela Dam on the River Indus, Water Res. Management 14 (2000) 191-208.

[24] S. Guillot, E. Garzanti, D. Baratoux, D. Marquer, G. Mahéo, De Sigoyer J., Reconstructing the total shortening history of the NW Himalaya, Geochem. Geophys. Geosyst. 4 (2003) 10.1029/2002GC000484

[25] P.J. Treloar, M.G. Petterson, M.Q. Jan, M.A. Sullivan, A re-evaluation of the stratigraphy and evolution of the Kohistan arc sequence, Pakistan Himalaya: Implications for magmatic and tectonic arc-building processes, J. Geol. Soc. London 153 (1996) 681-693

[26] Y. Rolland, A. Pêcher, C. Picard, Middle Cretaceous back-arc formation and arc evolution along the Asian margin : the Shyok Suture Zone in northern Ladakh (NW Himalaya), Tectonophysics 325 (2000) 145-173.

[27] P.R. Hildebrand, S.R. Noble, M.P. Searle, D.J. Waters, R.R. Parrish, Old origin for an active mountain range: Geology and geochronology of the eastern Hindu Kush, Pakistan, Geol. Soc. Am. Bull. 113 (2001) 625-639.

[28] M. Gaetani, The Karakorum Block in Central Asia, from Ordovician to Cretaceous, Sedim. Geol. 109 (1997) 339-359.

[29] A. Zanchi, D. Gritti, Multistage structural evolution of Northern Karakorum (Hunza region, Pakistan), Tectonophysics 260 (1996) 145-165.

[30] F. Debon, P. Le Fort, D. Dautel, J. Sonet, J.L. Zimmermann, Granites of western Karakorum and northern Kohistan (Pakistan) : a composite mid-Cretaceous to upper Cenozoic magmatism, Lithos 20 (1987) 19-40.

[31] M.P. Searle, Cooling history, erosion, exhumation, and kinematics of the Himalaya-Karakorum-Tibet orogenic belt, in: A.Yin, T.M. Harrison (eds.), The tectonic Evolution of Asia, Cambridge Univ. Press, 1996, pp. 110-137.

[32] D.A. Foster, A.J.W. Gleadow, G. Mortimer, Rapid Pliocene exhumation in the Karakoram (Pakistan), revealed by fission-track thermochronology of the K2 gneiss. Geology 22 (1994) 19-22

[33] E. Garzanti, T. Van Haver T., The Indus clastics: forearc basin sedimentation in the Ladakh Himalaya (India), Sedim. Geol. 59 (1988) 237-249.

[34] K. Honegger, P. Le Fort, J. Mascle, J.-L. Zimmermann, The blueschists along the Indus Suture Zone in Ladakh, NW Himalaya, J. Metam. Geol. 7 (1989) 57-72.

[35] M. Gaetani, E. Garzanti, Multicyclic history of the northern India continental margin (NW Himalaya), Am. Ass. Petr. Geol. Bull., 75 (1991) 1427-1446.

[36] A. Steck, Geology of the NW Indian Himalaya. Eclogae Geol. Helvetiae 96 (2003) 147-196.

[37] J.C. Vannay, B. Grasemann, M. Rahn, W. Frank, A. Carter, V. Baudraz, M. Cosca, Miocene to Holocene exhumation of metamorphic crustal wedges in the NW Himalaya: evidence for tectonic extrusion coupled to fluvial erosion, Tectonics 23 (2004), TC1014, 10.1029/2002TC001429.

[38] T. Argles, G. Foster, A. Whittington, N. Harris, M. George, Isotope studies reveal a complete Himalayan section in the Nanga Parbat syntaxis. Geology 31 (2003) 1109-1112.

[39] D.A. Schneider, P.K. Zeitler, W.S.F. Kidd, M.A. Edwards, Geochronological constraints on the tectonic evolution and exhumation of Nanga Parbat, Western Himalayan Syntaxis, revisited, J. Geol. 109 (2001) 563-583.

[40] A. Whittington, Exhumation overrated at Nanga Parbat, northern Pakistan, Tectonopysics 206 (1996) 215-226.

[41] M.A. Moore, P.C. England, On the inference of denudation rates from cooling ages of minerals, Earth Planet. Sci. Lett. 185 (2000) 265-284.

[42] D.W. Burbank, J. Leland, E. Fielding, R.S. Anderson, N. Brozovic, M.R. Reid, M.R., R. Duncan, Bedrock incision, rock uplift and threshold hillslopes in the northwestern Himalayas, Nature 379 (1996) 505-510.

[43] J.P. Burg, Y. Podladchikov, From buckling to asymmetric folding of the continental lithosphere: numerical modelling and application to the Himalayan syntaxes, Geol. Soc. London Spec. Publ. 170 (2000) 219-236.

[44] J.A. DiPietro, K.R. Pogue, A. Hussain, I. Ahmad, Geologic map of the Indus Syntaxis and surrounding area, northwest Himalaya, Pakistan. Geol. Soc. Am. Spec. Pap. 328 (1999) 159-178.

[45] K.R. Pogue, M.D. Hylland, R.S. Yeats, W.U. Khattak, A. Hussain, Stratigraphy and structural framework of Himalayan foothills, northern Pakistan. Geol. Soc. America Spec. Pap. 328 (1999) 257-274.

[46] M.S. Badshah, E. Gnos, M.Q. Jan, M.I. Afridi, Stratigraphy and tectonic evolution of the northwestern Indian plate and Kabul Block. Geol. Soc. London Spec. Publ. 170 (2000) 467-475.

[47] D.W. Burbank, R.A. Beck, T. Mulder, The Himalayan foreland basin, in: A.Yin, T.M. Harrison (eds.), The tectonic Evolution of Asia, Cambridge Univ. Press, 1996, pp. 149-188.

[48] M. Bernard, B. Shen-Tu, W.E. Holt, D.M. Davis, Kinematics of active deformation in the Sulaiman Lobe and Range, Pakistan, J. Geophys. Res. 105 (2000) 13253-13279.

[49] M. Qayyum, R.D. Lawrence, A.R. Niem, Molasse-delta-flysch continuum of the Himalayan Orogeny and closure of the Paleogene Katawaz remnant ocean, Pakistan (Int. Geol. Review 39 (1997) 861-875.

[50] E. Gnos, A. Immenhauser, T. Peters, Late Cretaceous/Tertiary coonvergence between the Indian and Arabian plates recorded in ophiolites and related sediments, Tectonophysics 271 (1997) 1-19.

[51] P.D. Warwick, E.A. Johnson, I.H. Khan, Collision-induced tectonism along the northwestern margin of the Indian subcontinent as recorded in the Upper Paleocene to Middle Eocene strata of central Pakistan (Kirthar and Suleiman Ranges), Palaeogeogr. Palaeoclimat. Palaeoecol. 142 (1998) 201-216.

[52] R. Anczkiewicz, J.P. Burg, I.M. Villa, M. Meier, Late Cretaceous blueschist metamorphism in the Indus Suture Zone, Shangla region, Pakistan Himalaya, Tectonophysics 324 (2000) 111-134.

[53] G.J. Weltje, End-member modelling of compositional data: numerical-statistical algorithms for solving the explicit mixing problem. J. Math. Geol. 29 (1997) 503-549.

[54] E. Garzanti, G. Vezzoli, S. Andò, C. France-Lanord, S.K. Singh, G. Foster G., Sand petrology and focused erosion in collision orogens: the Brahmaputra case, Earth Planet. Sci. Lett. 220 (2004) 157-174.

[55] G. Vezzoli, E. Garzanti, S. Monguzzi, Erosion in the Western Alps (Dora Baltea basin): 1.Quantifying sediment provenance, Sedim. Geol. 171 (2004) 227-246.

[56] M.J. Johnsson, R.F. Stallard, Lundberg N., Controls on the composition of fluvial sands from a tropical weathering environment: Sands of the Orinoco River drainage basin, Venezuela and Colombia, Geol. Soc. Am. Bull. 103 (1991) 1622-1647.

[57] E. Garzanti, S.Andò, Heavy mineral concentration in modern sands: implications for provenance interpretation, in: M. Mange, D. Wright (eds.), Heavy Minerals in Use, Developments in Sedimentology Series, Elsevier, in press.

[58] D. Jipa, R.B. Kidd, Sedimentation of coarser-grained interbeds in the Arabian Sea and sedimentation processes of the Indus Cone, Initial DSDP Report 23 (1974) 471-495.

[59] T.K. Mallik, Mineralogy of deep-sea sands of the Indian Ocean, Marine Geol. 27 (1978) 161-176.

[60] C.A. Suczek, R.V. Ingersoll, Petrology and provenance of Cenozoic sand from the Indus cone and the Arabian Basin, DSDP Sites 221, 222, and 224, J. Sedim. Petr. 55 (1985) 340-346

[61] M.E. Brookfield, The evolution of the great river systems of southern Asia during the Cenozoic India-Asia collision: rivers draining southwards, Geomorphology 22 (1998) 285-312.

[62] S.K. Singh, C. France-Lanord, Tracing the distribution of erosion in the Brahmaputra watershed from isotopic compositions of stream sediments, Earth Planet. Sci. Lett. 202 (2002) 645-662.

[63] E. Garzanti, G. Vezzoli, B. Lombardo, S. Andò, E. Mauri, S. Monguzzi, M. Russo, Collision-Orogen Provenance (Western and Central Alps): Detrital Signatures and Unroofing Trends, J. Geol. 112 (2004) 145-164.

[64] G. J. Weltje, Quantitative analysis of detrital modes: statistically rigorous confidence methods in ternary diagrams and their use in sedimentary petrology, Earth Sci. Rev. 57 (2002) 211-253

FIGURE CAPTIONS

Figure 1. Geological sketch map, indicating studied tributaries of the Indus River and sampled sites.

Figure 2. Bulk petrography (**A**) and heavy-mineral assemblages (**B**) of detritus carried by the Indus River and its major tributaries. Indus sands, rich in feldspars and amphiboles derived from both Asian active-margin batholiths and upper-amphibolite-facies young metamorphic massifs exposed around the Western Himalayan Syntaxis, plot near the boundary between "Recycled Orogen" (RO), "Magmatic Arc" (MA) and "Continental-block" (CB) provenance fields [14]. 90% confidence regions about the mean calculated after [64]; fields for Transhimalayan Arcs, Greater Himalaya, and Lesser Himalaya calculated with additional data from central and eastern Himalaya [54, own data]. Indices explained in Table 1.

Figure 3. Successive compositional changes in the Indus mountain catchment. Detrital modes of Indus sands change markedly downstream of each major confluence as the syntaxis is approached. Note invariably subordinate supply from rivers draining the Transhimalayan arcs (e.g., upper Indus, upper Shyok, Gilgit, Swat) with respect to tributaries draining the glaciated Himalaya and Karakorum-Hindukush mountains (e.g., Zanskar, Hushe, Hunza, Kabul). Symbols as in Fig. 2.

Figure 4. The effect of chemical weathering on detrital modes. The abundance of soluble carbonate grains (Lc) is roughly similar in the mountain catchment of the three big Himalayan rivers. Instead, across the foreland basin where rainfall increases markedly from arid Pakistan in the west (<250 mm/yr) to monsoon-drenched Assam in the east (1500-3000 mm/yr), carbonate grains remain common in Indus sands (indicating negligible dissolution), drop rapidly but survive in Ganga sands (to increase again downstream of the Gandak confluence; own data), and rapidly disappear in Brahmaputra sands [54]. Exponential regressions and correlation coefficients are shown for the Indus (pre-Kirthar Range), Ganga (pre-Gandak confluence) and Brahmaputra sands.

Figure 5. Quasi-symmetrical model for Himalayan sediment transport. If big dams built in the tightly regulated Indus basin virtually stop sediment discharge, detritus sequestered in reservoirs can be measured

and upstream sediment flux thus effectively constrained. WHS = Western Himalayan Syntaxis (Nanga Parbat Massif and adjacent South Karakorum Belt; ~12,600 km^2; sediment yield 10,900±4400 t/km^2 yr); EHS = Eastern Himalayan Syntaxis (Namche Barwa Massif; ~27,000 km^2; sediment yield 8900±4400 t/km^2 yr [54,62]).

Figure 6. The effect of active-margin sources and focused erosion of young metamorphic massifs on detrital modes. **A**) Indus and Brahmaputra sands are much richer in feldspars and amphiboles than those of all other major Himalayan rivers from Pakistan to Assam (empty squares; own data). Brahmaputra field includes only pre-Ganga samples. **B**) Signatures of Indus sands largely reflect active erosion of both Asian-margin batholiths and upper-amphibolite-facies middle-crustal domes at the Western Himalayan Syntaxis. 90% confidence regions for the entire population (A) and about the population mean (B) calculated after [64]. Indices as in Table 1, symbols as in Fig. 2.

Table 1. Key Indices for Framework Composition and Heavy-Mineral Suites.
Framework composition and P/F ratio determined by the Gazzi-Dickinson QFL method [13,14]; other ratios by the traditional QFR method. HMC = "Heavy Mineral Concentration index" of [57].

Table 2. Bulk petrography and heavy-mineral assemblages in selected modern Indus sands.
N= number of samples. Indices as in Table 1. For the complete database (including another 16 samples from Indus River, 8 samples from Punjab tributaries, and several others from tributaries with mixed provenance) the reader is referred to Appendices A1 and A2 available in the online edition of EPSL and from the EPSL Data Depository upon request.

APPENDICES

(available in the online edition of EPSL and from the EPSL Data Depository upon request)

APPENDIX A1

Table A1 Detrital Modes of Modern Sands in the Indus River Basin.

Q= quartz; F= feldspars; Lv= volcanic lithic fragments; Lc= carbonate lithic fragments; Lp= pelitic terrigenous lithic fragments; Lch= chert lithic fragments; Lm= metamorphic lithic fragments; Lu= ultramafic lithic fragments. Qp= polycrystalline quartz; P= plagioclase. Rim/i= mafic and intermediate plutonic rock fragments/total plutonic rock fragments; Rvm/v= mafic and intermediate volcanic and subvolcanic rock fragments/total volcanic and subvolcanic rock fragments; Rcd/c= dolostone rock fragments/total carbonate rock fragments; Rmb/m= metabasite rock fragments/total metamorphic rock fragments; Ruc/u= massive cellular serpentinite and preserved peridotite rock fragments/total ultramafic rock fragments. MI= "Metamorphic Index" [15], defined as the weighted sum of the relative percentage of very low-rank (e.g., slate), low-rank (e.g., phyllite), medium-rank (e.g., very fine-grained micaceous schist), high-rank (e.g., fine-grained muscovite schist), very high-rank (e.g., coarse-grained muscovite-biotite schist) metamorphic grains. The MI index ranges from 100 (only very low-rank lithic fragments) to 500 (only very high-rank rock fragments). Key indices and P/F ratio calculated by the Gazzi-Dickinson point-counting method; other ratios by the traditional QFR method; n.d.= not determined. GSZ= median diameter, determined by ranking and direct measurement in thin section. Percent micas and heavy minerals (HM) calculated on total framework grains.

APPENDIX A2

Table A2 Transparent Heavy Minerals in Modern Sands of the Indus River Basin.

HMC = "Heavy Mineral Concentration index" [57], defined as the weight percentage of heavy minerals (transparent, opaque, and turbid grains denser than 2.90 g/cm^3) in the 63-250 μm terrigenous extrabasinal fraction of studied samples. HCI= "Hornblende Color Index"[63], defined as the weighted sum of the relative percentage of blue-green, green, green-brown, and brown hornblende grains. The HCI index ranges from 0 (only blue-green hornblende) to 100 (only brown hornblende). MMI = "Metasedimentary Mineral Index" [57], defined as the weighted sum of the relative percentage of four index minerals found in low-grade to high-grade metasediments (chloritoid, staurolite, kyanite, and sillimanite). The MMI index

ranges from 0 (only chloritoid) to 100 (only sillimanite). Grain size determined by sieving; n.d.= not determined.

APPENDIX A3

Table A3 Calculated end-member contributions and analysis of variance for the Indus River mountain catchment upstream of Tarbela Dam.

The example illustrates the joint use of source terrains and big tributaries as end-members. The robustness of the results obtained can be checked through repeated calculations with different choices of end-members. Matrix X (11, 30) includes 11 observations (observed compositional signatures of selected end-members) and 30 variables (most significant petrographic and mineralogical parameters). Row vectors y and $\hat{y}$ (1, 30) include 30 variables (observed and calculated composition of Indus River sand upstream of Tarbela Dam). Row vector b (1,11) includes 11 coefficients (estimated proportional contribution of each end-member to the Indus River sand). RSS = residual sum of squares; MSS = model sum of squares, R^2 = coefficient of determination. F = Fischer statistic test; F_{crit} = F values determined via standard lookup tables for 5% and 1% probability.